ORIGINAL PAPER

Kinetics and yields of bacteriochlorophyll fluorescence: redox and conformation changes in reaction center of *Rhodobacter sphaeroides*

Péter Maróti

Abstract Induction of the bacteriochlorophyll fluorescence under rectangular shape of intense laser diode illumination (1 W cm^{-2}, 808 nm) was measured over wide time range from 10 μs to 4 s in whole cells, chromatophore and isolated reaction center protein of wild type and carotenoid-less mutant (R-26.1) of purple photosynthetic bacterium *Rhodobacter sphaeroides*. While the antenna-containing species showed large and positive variable fluorescence (F_v) to initial fluorescence (F_0) ($F_v/F_0 \sim 4.5$ in whole cells), the isolated RC had negative change ($F_v/F_0 \sim -0.6$) during photochemistry. In chromatophore from R-26.1, only seven times higher rate was measured than in isolated reaction center under identical experimental conditions. The enhancement effect of large antenna on the rate of photochemistry in chromatophore was partially compensated by the favorable pigment absorption properties in isolated RC. The transition from membrane bound to isolated form of the reaction center was probed by titration of zwitterionic detergent LDAO in chromatophore, and at 0.03% LDAO concentration, sharp change of the variable fluorescence was observed. The sudden drop was explained by the formation of LDAO micelles. After the photochemical phase, additional change of fluorescence yield could be observed in isolated RC considered as manifestation of long-living conformations of the trapped redox states of the protein characterized by non-exponential kinetics. Strong support was provided for

use of the fluorescence induction to track structural and conformation changes at their earliest phases in chromatophores and isolated reaction centers.

Abbreviations

BChl	Bacteriochlorophyll
Bpheo	Bacteriopheophytin
D	External electron donor to P$^+$
F_0	Initial fluorescence intensity
F_v	Variable fluorescence intensity
LDAO	*N,N*-dimethyldodecylamine-*N*-oxide
LH I and LH II	Light harvesting complexes I and II, respectively
P	Bacteriochlorophyll dimer
PSII	Photosystem II of higher plants
Q	Quinone acceptor
Q_A	Primary quinone acceptor
Q_B	Secondary quinone acceptor
RC	Reaction center protein
UQ$_{10}$	Ubiquinone-50

P. Maróti (✉)
Department of Biophysics, University of Szeged,
Egyetem utca 2, 6723 Szeged, Hungary
e-mail: pmaroti@sol.cc.u-szeged.hu

Introduction

In photosynthetic organisms, the captured light covers the costs of energy to produce useful chemical products. Although the overall yield of the energy conversion is low (1–2%), the yield of the initial photophysical processes [absorption of the light by the antenna, funnel of the electronic excitation energy to the reaction center (RC)

protein and the primary charge separation] is high: e.g. close to 100% of the excited (bacterio)chlorophyll (BChl) dimer of the RC (P*) makes charge separation (Wraight and Clayton 1974). The efficient photophysics is due mainly to the optimal selection of the spectroscopic properties of the pigments and their organization in the antenna system and in the RC.

The photosynthetic apparatus of the bacterium *Rhodobacter* (*Rba.*) *sphaeroides* (wild type) consists of three membrane-bound pigment–protein complexes: light-harvesting complexes I (LH I or B875) and II (LH II or B800–850), and the RC, along with the associated components required for subsequent electron transport and energy transduction. The LH II antenna complex of the carotenoidless mutant of *Rba. sphaeroides* (R-26.1) is similar in polypeptide composition to the wild-type B800–850-complex, but lacks both carotenoids and the 800-nm absorbing bacteriochlorophyll. Approximately 14 LH I complexes surround and contact the RC, whereas the LH II complexes are positioned around the B875-RC complex (Cogdell et al. 2003; Roszak et al. 2003). The pigment–protein complexes B875 and B800–850 harvest solar energy and funnel it to the RC. The functional core of the RC complex is a heterodimer of two (L and M) subunits that bind all the active cofactors: four BChls, two bacteriopheophytins (Bpheo), two quinones, and one non-heme iron atom. The third (H) subunit stabilizes the whole complex and is involved in proton binding and electron transfer between the two quinones. The arrangement of the cofactors and protein subunits exhibits a high degree of rotational symmetry, well known from the X-ray structures of RC complexes from several species (see Wraight 2004).

Upon direct absorption of the light or transfer of the electronic excitation energy from the antenna, the BChl dimer (P) will be excited (P → P*). Within 2–4 ps, charge separation occurs (P* → P$^+$Bpheo$^-$) followed by electron transfer along the active branch via Q_A (150–200 ps) to Q_B (10–100 μs), the stable primary and secondary quinone acceptors, respectively. In spite of the structural symmetry, only one branch (A) is active in electron transfer. The light-separated charges may recombine (P$^+$Q$^-$ → PQ) from Q_A^- and Q_B^- (via Q_A) within 100 ms and 1 s, respectively. If external electron donor (D) re-reduces P$^+$ - (DP$^+$Q$^-$ → D$^+$PQ$^-$) faster than the charge recombination, then the quinone acceptors will be trapped in long-living semiquinone states P($Q_A Q_B$)$^-$. The semiquinone and oxidized dimer states can facilitate changes of the conformation of the protein manifested in charge recombination kinetics (Kálmán and Maróti 1997; Andréasson and Andréasson 2003; Agostiano et al. 2005; Katona et al. 2005), proton uptake (Kálmán and Maróti 1997), magnetic properties (Mueh et al. 1997) or protein dynamics (McMahon et al. 1998; van Mourik et al. 2001; Goushcha

et al. 2004; Breton et al. 2007). The observed effects are mostly induced by long illumination and possibly include wide variety of slight structural changes.

Although the pigments in the light harvesting system and in the RC are tightly packed and energetically well coupled, small part of the transferred energy is dissipated in form of (bacterio)chlorophyll fluorescence. Its detection can be used to monitor internal excitation and electron transfer processes. If the photosynthetic organism is exposed to sudden change from dark to light of constant intensity, complex kinetics of the (bacterio)chlorophyll fluorescence (fluorescence induction) can be observed. The phenomenon was discovered by Müller (1874) and studied for the first time by Kautsky and Hirsch (1931) in oxygenic phototrophs and by Vredenberg and Duysens (1963) in anoxygenic phototropic purple bacteria. It has become one of the most frequently used tools in photosynthesis research of green plants to study the organization of the light harvesting system and the molecular mechanisms of energy capture and conversion to chemical energy (Dau 1994; Papageorgiou and Govindjee 2004; Lazar 2006; Cser and Vass 2007). In comparison with chlorophyll fluorescence, the use of fluorescence induction of bacteriochlorophyll is much more limited, probably due to the widespread use of kinetic absorption spectrometers to monitor the redox reactions in photosynthetic bacteria (Osváth et al. 1996; Trissl 1996, 1999; Koblizek et al. 2005; Gerencsér and Maróti 2007).

In this work, we show that, despite the experimental difficulties, the fluorescence induction in bacterial systems can be made as informative as it is in higher plants. Kinetic traces of fluorescence induction in whole cells, chromatophores and isolated RC of the carotenoidless mutant of *Rba. sphaeroides* (R-26.1) were measured in wide time range from 10 μs to 4 s under rectangular shape of intense illumination. Different phases of the fluorescence induction kinetics were used to track the gradual solubilization of the RC by detergent from the membrane and to probe minor conformation changes of the RC after charge separation.

Materials and methods

Sample preparation

The cells of the wild (2.4.1) and carotenoidless mutant (R-26.1) of the photosynthetic bacterium *Rhodobacter* (*Rba.*) *sphaeroides* were anaerobically cultivated under 13 W m^{-2} light intensity offered by tungsten lamps (40 W). Chromatophores (membrane fragments) were obtained by mechanical rupture (sonication) of the cells harvested in the stationary phase of the growth as described previously (Maróti and Wraight 1988). By this procedure, most of the

water-soluble cytochrome c_2 were lost. The chromatophores were used immediately or kept at $-14°C$ in a glycerol-containing (60:40 v/v) buffer (50 mM sodium glycyl-glycine) at pH 8. The concentration of BChl was determined spectroscopically following extraction in polar solvents (acetone/methanol, 7:2 v/v) by use of the extinction coefficient of 75 mM^{-1} cm^{-1} at 770 nm. Typical BChl concentrations of the samples were 30 μM. The RC protein was isolated from chromatophore by standard procedure reported earlier (Maróti and Wraight 1988). During preparation, the secondary quinone activity of the RC was partly lost but could be reconstituted by addition of UQ$_{10}$ solubilized in Triton X-100 non-ionic detergent ($\sim$2Q/RC). The concentration of the RC was determined from flash-induced absorption change at 430 nm using extinction coefficient of 26 mM^{-1} cm^{-1} (see for details in Maróti and Wraight 1988). The RC concentrations were approximately 1 μM. Terbutryne was used to block the interquinone electron transfer and ferrocene to re-reduce the photooxidized dimer (P$^+$) of the RC. All measurements were done at room temperature and pH 8.

Fluorescence measurements

The kinetics and yield of the bacteriochlorophyll fluorescence upon rectangular shape of illumination were recorded by a home-built spectrofluorometer with laser diode excitation (808 nm, 1 W cm^{-2}) (Fig. 1). The duration and intensity of the laser pulse could be adjusted by a control unit (digital pulse generator, Híradástechnika, TR-0360/0007). The attenuation of the laser intensity was calibrated by neutral density filters. The rise time of the laser excitation was much less than the time resolution of the device ($\sim$1 μs) and the flash of the laser diode formed the shape of a step function with good approximation. In addition to the laser diode, the sample could be excited by saturating laser flash from a frequency-doubled and Q-switched Nd:YAG laser (Quantel YG 781.10, wavelength 532 nm, duration 5 ns and energy 100 mJ). The fluorescence of the sample was detected at 90° with respect to the excitation light through an IR cutoff filter (Schott RG-850, $\lambda > 850$ nm) and, in case of RC, through an interference filter ($\lambda = 916 \pm 15$ nm). There is a small spectral shift in fluorescence: the peaks of the fluorescence are 890 and 916 nm for the antenna and the RC, respectively (De Klerk et al. 1969; Osváth et al. 1996). The red-sensitive photomultiplier tube (Hamamatsu R3310-03) was cooled down to $-30°C$ (Photocool PC 410CE; Products for Research) to reduce the dark current by 2–3 orders of magnitude and to increase the signal/noise ratio (S/N). The fluorescence kinetics were detected and transiently stored in a digital oscilloscope (Tektronix 3032, 300 MHz, 2.5 GS s^{-1}) and were transferred to a personal computer for storage and
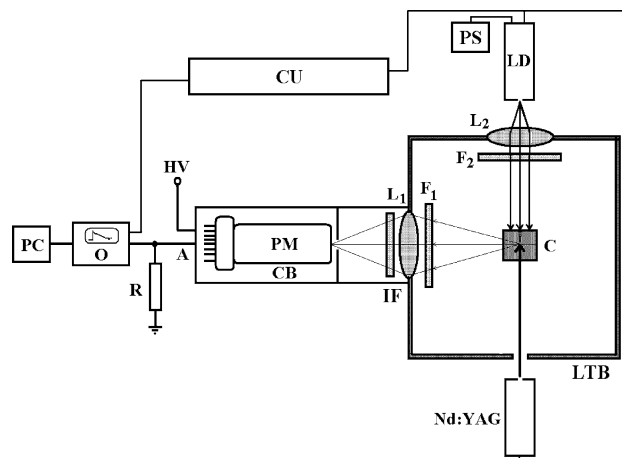

Fig. 1 Schematic view of the optical and electronic arrangement of bacteriochlorophyll fluorometer to measure kinetics and relative yield of fluorescence excited by of laser diode (*LD*) and Nd:YAG laser flash in photosynthetic bacteria. Symbols: *PC* personal computer, *O* digital oscilloscope, *R* load resistance, *A* anode, *HV* high voltage, *PM* photomultiplier, *CB* cooling box, L_1 and L_2 lenses, F_1 and F_2 optical (*red*) cutoff filters ($\lambda > 850$ nm), *IF* interference filter ($\lambda = 916 \pm 15$ nm), *C* cuvette, *LTB* light-tight-box, *CU* control unit, *PS* power supply

analysis. The traces of dark-adapted samples were recorded after single illumination. In case of low S/N, however, a couple of measurements (typically 4–8) always with fresh samples were averaged. The kinetic trace of the fluorescence from the sample was divided by that of the laser diode emission to eliminate any effects of minor temporal changes of the laser diode excitation on the observed fluorescence. The fluorescence was normalized to its initial value determined at attenuated light excitation when the constant (F_0) and variable (F_v) parts of the fluorescence could be kinetically well separated. The optical densities of the samples in a 1×1 cm rectangular quartz cuvette were kept low [OD (865 nm) < 0.4] to minimize the secondary effects (scattering, re-absorption of BChl fluorescence, secondary fluorescence, etc.).

The flash-induced kinetic traces were decomposed into exponential functions using non-linear least-square fitting. The set of differential equations derived from Scheme 1 to simulate data in Fig. 4A and Eqs. (3) and (4) to fit data in Fig. 5 were solved numerically by MathCad 4.0.

Results

It is well known that the yield of fluorescence of BChl *a* in vitro (in solution) does not show temporal changes upon excitation of moderate light intensity. On the contrary, BChl *a*-containing photosynthetic organisms do demonstrate complex time-courses of the fluorescence upon dark-to-light transition (fluorescence induction). The fastest

phase of the fluorescence induction is the photochemical phase, whose rate and sign of change are controlled by the exciting light intensity and the organization of the pigments participating in collection of excitation energy and in emission of the fluorescence. This can be demonstrated by tracking the fluorescence induction kinetics in different organization levels of the bacterium under different light regimes.

Significantly different fluorescence kinetics can be observed in isolated RC, membrane fragments (chromatophores) and in whole cells (Fig. 2A). While the fluorescence increases in the antenna-containing species (whole cells and chromatophores), it decreases if the antenna is removed (isolated RC). By the end of the photochemical phase, the relative yields of fluorescence (F_v/F_0, where F_v is the variable fluorescence and F_0 is the initial fluorescence) becomes high for whole cells (>4) but less in chromatophore (≈ 2.5) or in isolated RC (−0.6). The negative sign indicates the decrease of variable fluorescence in isolated RC.

The photochemical character of the fluorescence change can be confirmed in two different ways. In isolated RC, a saturating short flash from the Nd:YAG laser was fired just before the initiation of the rectangular illumination of the laser diode (1 µs, Fig. 2B). As a consequence of the saturating pre-flash, the fluorescence induction disappeared completely and the yield of fluorescence showed constant value that was close to the limiting yield measured under identical conditions but without Nd:YAG laser flash. The whole phase could be knocked out by a single saturating flash.

The change of the rate of the rise (chromatophore) or decay (RC) with light intensities is indicative of the photochemical nature of the phase (Maróti and Lavorel 1979; Trissl 1999; Fig. 2C). Attenuation of the exciting light

intensity was achieved by calibrated neutral density filters. In double logarithm representation, straight lines with slopes close to 1.0 were obtained for both chromatophores and isolated RC from R-26.1, indicating that only photochemical reactions determine the rise (chromatophore) and decay (RC) of the fluorescence in this time range. As the conditions for excitation ($\lambda = 808$ nm) and observation ($\lambda > 850$ nm) were the same (there is only slight difference in spectral properties of the fluorescence from the antenna and the RC, see M@M), the ratio of the observed rates
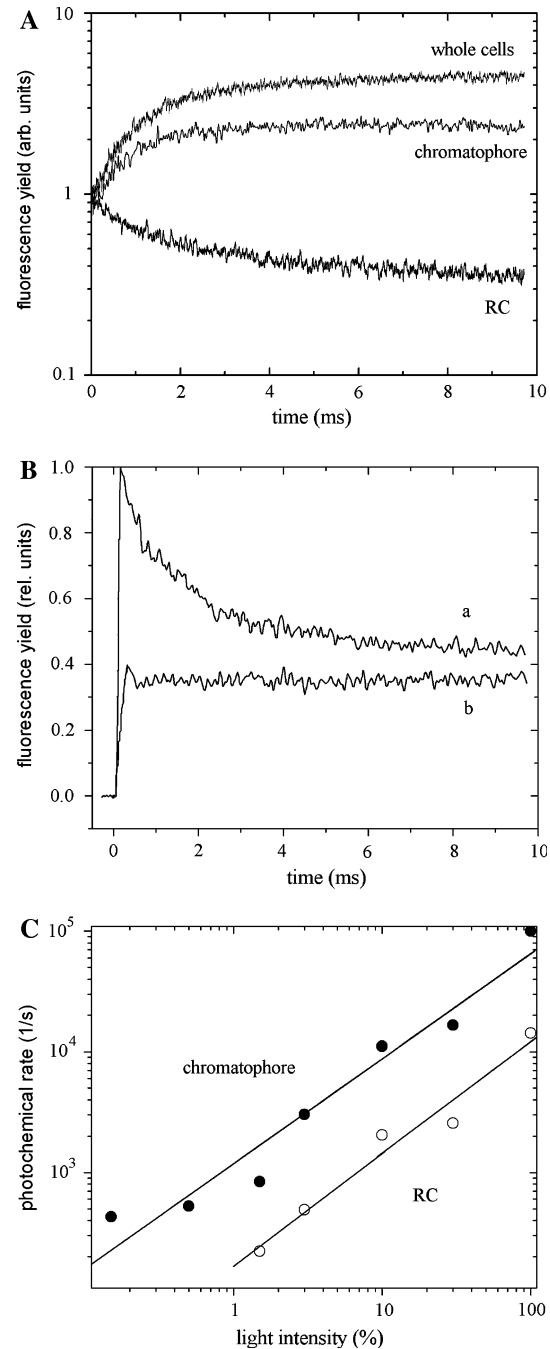

Fig. 2 Photochemical phase of bacteriochlorophyll fluorescence induction in whole cells, chromatophore and isolated RC upon rectangular laser diode excitation. A Kinetics of the relative yield of fluorescence. The samples were illuminated by different light intensities (typically 10 mW cm^{-2}) to adjust the photochemical (excitation) rates to the same time scale and the kinetic traces were normalized to the same initial value. Note the logarithmic scale of the fluorescence yield. B Disappearance of the photochemical phase by saturating pre-flash in isolated RC. The fluorescence induction was monitored without (a) and with (b) saturating Nd:YAG laser flash fired 1 µs before the onset of the laser diode excitation. Conditions: 2 µM RC, 0.03% Triton X-100, 2 mM Tris, pH 8 and 120 µM terbutryne. C Comparison of the rates of the photochemical phase of the fluorescence induction excited by the same light intensities in chromatophores (filled circle) and isolated RCs (open circle) from R-26.1. The light intensities of excitation were attenuated by calibrated neutral density filters and the fluorescence of the sample was detected through RG-850 cutoff filter. Note the double logarithmic representation, where the slopes are 0.87 (chromatophore) and 0.93 (RC) and the rate is seven times higher in chromatophore than in isolated RC under identical light intensity
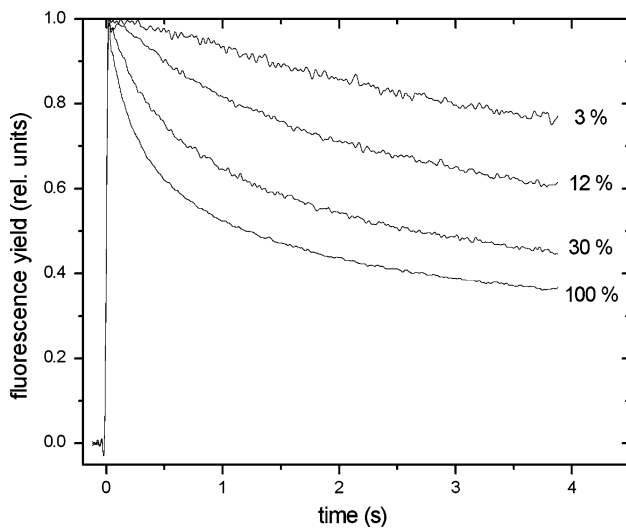
Fig. 3 Long term and light-intensity dependent quenching of the bacteriochlorophyll fluorescence in whole cells of bacteria of carotenoid deficient mutant (R-26.1). The kinetic traces were taken under different light intensities attenuated by calibrated neutral density filters. At excitation of 100% light intensity, the rate constant of the photochemical rise was $1 \times 10^4 \text{ s}^{-1}$

should be characteristics of the antenna function. Under these conditions, the presence of the antenna complex in chromatophore from carotenoid-less mutant (R-26.1) assured only seven times higher rate of the photochemistry than in isolated RC.

After the photochemical rise, the yield of the fluorescence reaches stationary level. If, however, the illumination is intense and long, the fluorescence starts to be quenched as observed in whole cells of carotenoidless (R-26.1) mutant of the bacteria (Fig. 3). The larger the light intensity, the more pronounced the decay of the yield of fluorescence observed in the second time range. The quenching is not a linear function of the light intensity (see Maróti and Lavorel 1979). The drop of the fluorescence is not attributed to the possible non-linearity of the detection system as can be seen from the following experiment. The same filter of low (3%) transmittance is placed first in the excitation light path and then in the detection light path. Although in both cases, the load of the detector (photomultiplier) remained the same (figure not shown), quenching of fluorescence was observed in the latter but not in the first case. Consequently, the drop of the yield of fluorescence upon increase of the light intensity is not an artifact but comes from the sample. The decrease of the fluorescence yield can be connected to energetization of the membrane and/or to damage of the pigments of the cell (photobleaching).

Under similar conditions, the fluorescence is not quenched in isolated RC from wild-type bacteria, where the carotenoids can protect the excited bacteriochlorophylls

against harmful attack of oxygen molecules (Fig. 4A). After onset of the excitation (the yield takes its initial value within 10 μs) and implementation of the photochemical phase ($\sim$10 ms), the change of the yield of fluorescence does not come to an end but increases (PQ_A^-) or decreases ($P^+Q_A^-$/terb and $P^+Q_B^-$) further.

The kinetic properties of the different redox states of the RC can be studied by monitoring the flash-induced absorption change at 430 nm (Fig. 4B). At this wavelength, the absorption change is dominated by the P/P^+ redox change but the Q/Q^- redox change has also some contributions (see the enhanced level of absorption (curve a) after P^+ is re-reduced by ferrocene). The time constant of P^+ re-reduction is smallest if ferrocene directly donates P^+ (3.0 ms) and larger via $P^+Q_A^- \rightarrow PQ_A$ (96 ms) and $P^+Q_B^- \rightarrow PQ_B$ (834 ms) charge recombinations. These kinetic data contribute to the interpretation of the complex kinetics of fluorescence induction in different redox states of the RC (Fig. 4A).

The phases of the fluorescence induction could serve as signature of organization of BChl pigments in the photosynthetic apparatus. The most demonstrative examples are the change of fluorescence characteristics during assembly (Koblizek et al. 2005) and age (De Klerk et al. 1969) of the photosynthetic unit and redox changes of the RC (Osváth et al. 1996). Here, we show how the numbers, connectivity or distribution of the pigments may change upon disturbance of the RC/membrane structure by LDAO, a zwitterionic detergent generally used to solubilize the RC from the membrane (Fig. 5). The fluorescence induction in the two time regimes had different behavior upon LDAO titration. The slow phase did not show changes, the mechanism that controls the drop of fluorescence yield was independent of the LDAO concentration. Contrary to that, the fast (photochemical) phase was highly sensitive to the detergent at specific concentration range. The variable fluorescence suddenly disappeared and altered its sign at 0.03% LDAO.

Discussions

The common belief is that the fluorescence induction is much more simple in photosynthetic bacteria than in green plants. Highly sophisticated chlorophyll kinetic fluorometers are on the market and play central role in study of photosynthesis of higher plants. By construction of a bacteriophlorophyll fluorometer, we showed that the fluorescence induction of photosynthetic bacteria could be similarly complex and informative as those observed in green plants. In different organization levels of the photosynthetic bacteria (whole cells, chromatophore and isolated RC) different kinetic phases could be distinguished
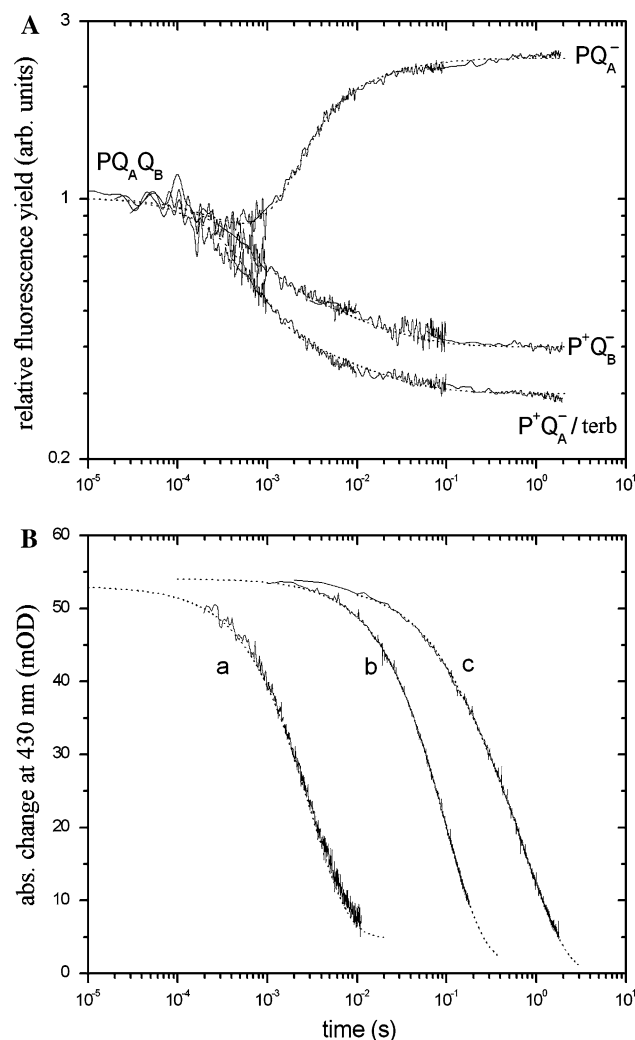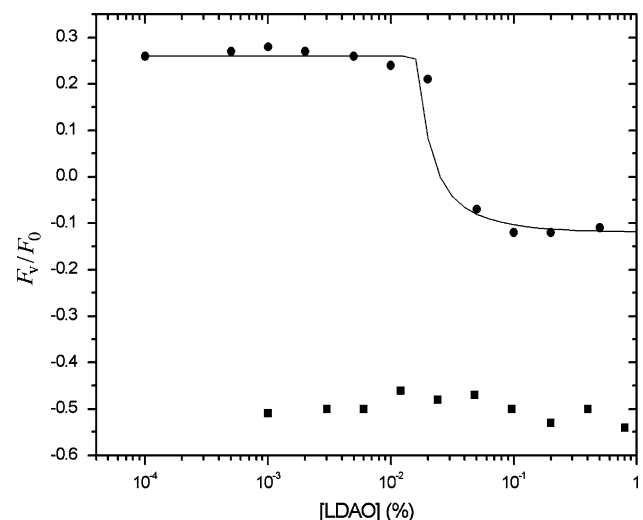
Fig. 5 Change of variable-to-initial fluorescence (F_v/F_0) for the fast (photochemical) (*filled circle*) and slow (*filled square*) phases in chromatophore upon titration of LDAO. The intensity of the exciting light of the laser diode provided fluorescence time constants of 20 μs and 0.5 s for the fast and slow phases, respectively. The samples received single pulses. The concentration of the stock solution of LDAO was 30%. The fitting curve to the drop of the variable fluorescence upon increase of LDAO concentration (*solid line*) was obtained by numerical solution of Eqs. (3) and (4) with cmc = 0.034% (1.48 mM), $N = 76$, $a = 0.26$, $b = -0.12$ and $K_{mic} = 2 \times 10^4$ 1/% (4.58×10^5 M^{-1})

induction can be used to monitor (1) the rates of photochemistry in chromatophore and isolated RC under identical conditions, (2) the solubilization of RC from the membrane by the detergent LDAO and (3) the redox and conformation changes of RC under continuous and strong illumination.

Comparison of rates of light utilization in chromatophore and isolated RC

The fastest phase of the fluorescence induction in our experiments was characteristic of the rate of utilization of the excitation energy for photochemistry (Fig. 2B). With application of two independent methods, we proved the photochemical nature of this phase. The rate of the change of the fluorescence was found proportional to the exciting light intensity. Higher rate of fluorescence increase (chromatophore) or decrease (isolated RC) under otherwise identical conditions would involve faster photochemistry or more efficient capture of the excitation by the photosynthetic apparatus.

The structure and effectiveness of the light-collecting systems of the chromatophore and solubilized RC protein are significantly different. Whereas extended pigment/protein complexes help to harvest the light excitation in chromatophore, the absorption cross-section is limited to a

Fig. 4 Kinetics of fluorescence induction excited by laser diode and flash-induced absorption changes of isolated RC. **A** Relative yield of bacteriochlorophyll fluorescence of isolated RC in different redox and conformation states. Please note the logarithmic scales. The *dotted lines* were calculated from Eq. (5) and Scheme 1 using rate constants of $k_I = 1{,}800$ s^{-1} (photochemistry), $k_r = 1.2$ s^{-1} and 10 s^{-1} (charge recombination of P$^+$Q$_B^-$ → PQ$_B$ and P$^+$Q$_A^-$ → PQ$_A$, respectively), $k_d = 330$ s^{-1} (electron donation by ferrocene to P$^+$) and $k_o = 1{,}000$ s^{-1} and $\alpha = 0.3$ (Kohlrausch relaxation function). The relative fluorescence yields were taken from Table 1. **B** Flash-induced absorption change (at 430 nm) of isolated RC in the presence of 200 μM ferrocene (*a*), 120 μM terbutryne (*b*) and 30 μM UQ$_{10}$ (*c*). Logarithmic time scale was used to demonstrate the very different kinetics of P$^+$ re-reduction by electron donation by ferrocene (*a*) or by charge recombination (*b*, *c*). *Dotted lines* are best-fit curves with exponential lifetimes of 3.0 ms (*a*), 96 ms (*b*) and 126 ms (fast component, amplitude 18%) and 834 ms (slow component, amplitude 82%) (*c*). Conditions: 2 μM RC, 0.03% Triton X-100, 2 mM Tris, pH 8, 2UQ$_{10}$/RC (P$^+$Q$_B^-$ redox state) or 120 μM terbutryne (P$^+$Q$_A^-$/terb redox state) or 200 μM ferrocene (PQ$_A^-$ redox state)

and used for sensitive probes of photochemistry, photobleaching, antenna organization and redox and conformation changes of the RC. The discussion will be restricted to three topics analyzing how the fluorescence

couple of internal pigments in isolated RC. The antenna fluorescence is usually much more intense than the RC fluorescence due mainly to two reasons: (1) the antenna has about 100 times more BChl pigments than the RC and (2) the quantum yield of the BChl fluorescence in the antenna (1–2%, van Grondelle and Duysens 1980, but 1×10^{-3}, Borisov and Godik 1972) is much larger than in the RC (4×10^{-4}, Zankel et al. 1968). The difference is due to the effectiveness of the photochemical trap in the two cases. Taking into account the size of the antenna, the excitation energy is funneled from about two orders of magnitude larger area in chromatophore than in isolated RC. The rates of photochemistry should reflect this ratio. However, we obtained only seven times larger rate in chromatophore than in isolated RC under identical conditions (Fig. 2C).

To understand our observation, we have to consider that the absorption cross-section is determined not only by the number of pigments but also by their absorption at the wavelength of excitation. The smaller rate of photochemistry than expected in chromatophore is due to the unfavorable wavelength of excitation. In our experiments, the wavelength of the laser diode excitation was 808 nm that matched the BChl monomers of the RC but not the LH II of R-26.1 that lacked the B800 pigment. Under this condition, the photochemical rise of the fluorescence induction of the chromatophore was only seven times faster than in isolated RC. From the point of view of the rate of light utilization, the large number (and strong coupling) of pigments in the antenna of the chromatophore was partly compensated by the favorable excitation of the RC pigments.

Fluorescence induction as probe for solubilization of RC from the membrane

The kinetics and yield of fluorescence are very sensitive to the organization of the pigments participating in the collection and trapping of the excitation energy. This can lead to opposite signs of the variable fluorescence in chromatophore and isolated RC (Fig. 2A). Conversion of the variable fluorescence from increasing to decreasing character can be expected upon removal of the protein from the membrane. Indeed, sharp transition was experienced upon titration of the zwitterionic detergent LDAO into the chromatophore (Fig. 5). The sudden change indicates the presence (binding) of critical number of LDAO molecules. Below that number, the connectivity of pigment molecules of the protein and antenna in the membrane is not affected but above this threshold, the connection (or one of the major coupling factors) breaks and the variable fluorescence is significantly modified.

The LDAO concentration of 0.021% (0.9 mM) is able to solubilize the RC from *Rba. sphaeroides* by forming a detergent belt around the protein consisting of about 150 LDAO molecules (Gast et al. 1996). This LDAO concentration needed to solubilize the protein is slightly below the critical micelle concentration (cmc) of LDAO (0.023%, Hermann 1962; 0.034%, Strop and Brunger 2005). Our value (0.03%) obtained from the sudden drop of the variable of fluorescence (Fig. 5) matches the cmc indicating that the micelle formation has abrupt effect on the fluorescence property of the RC embedded into the membrane. The observed value in Fig. 5 is 2–3 times lower than the LDAO concentration typically used for RC crystallization (0.1%, Gast et al. 1996) and is much lower than the concentration routinely applied to dissolve the RC from the membrane (0.65–1%, Maróti and Wraight 1988).

To work out the quantitative details of the unusually sharp transition, the mass action rule should be applied to the consecutive reactions of micelle formation of LDAO:

$$(N \text{ monomers}) \overset{\text{cmc}}{\leftrightarrow} (\text{one micelle}) \tag{1}$$

and to interaction of micelles with RC/membrane that leads to loose the RC/membrane structure, (RC/membr)′:

$$(\text{RC/membr}) + \text{micelle} \overset{K_{\text{mic}}}{\leftrightarrow} (\text{RC/membr})'. \tag{2}$$
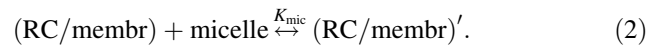
Here N is the aggregation number of the LDAO and K_{mic} is the binding constant of the LDAO micelles to the chromatophore (RC/membrane).

From reaction (1), we get

$$
[\text{LDAO}] = ([\text{LDAO}] - N \cdot [\text{mic}]) \\
\cdot \left(1 + \left(\frac{2 \cdot ([\text{LDAO}] - N \cdot [\text{mic}])}{\text{cmc}}\right)^{N-1}\right) \tag{3}
$$

where [LDAO] is the total concentration of LDAO introduced into the solution, [mic] is the concentration of the micelle and cmc is the critical micelle concentration. There is no analytic solution for the concentration of the micelles and numerical methods should be applied.

Reaction (2) includes hyperbolic relationship between fluorescence yield and concentration of micelles:

$$\frac{F_{\text{v}}}{F_0} = b + \frac{a - b}{1 + K_{\text{mic}} \cdot [\text{mic}]} \tag{4}$$

where a and b are the limiting fluorescence yields at very low and very high LDAO concentrations, respectively.

Equations (3) and (4) were used to fit the experimental results (Fig. 5). After taking cmc = 0.034% (1.48 mM) (Strop and Brunger 2005) and $N = 76$ (Hermann 1962; Gast et al. 1996), [mic] could be calculated from Eq. (3) at each [LDAO] values and replaced in Eq. (4). We got $a = 0.26$, $b = -0.12$ and $K_{\text{mic}} = 2 \times 10^4$ 1/% (4.58×10^5 M^{-1}) for the fitting parameters. Whereas the sharp initial drop of the fluorescence yield is correlated to the micelle formation, the final (stabilization) level of the

fluorescence is determined by the binding affinity of the micelle to the RC. The fitting procedure gave typical (not extreme) value for the binding constant.

Partly quantified explanation is given for the very sudden onset of the fluorescence drop. Certainly, more detailed analysis is needed to obtain precise description of the effect of LDAO on the BChl fluorescence in membrane, but we can extract important lessons from this simplified treatment, as well. First, the drop of the variable fluorescence comes from the formation of LDAO micelles. Second, the fluorescence induction probes the intactness of the RC/membrane structure and indicates its perturbation much before the collapse of this ordered arrangement. Third, the cooperativeness and proper geometrical packing of LDAO molecules and RC/membrane sharpen the transition, mitigating all other effects including random thermal motion and structural heterogeneity.

Fluorescence induction as probe for redox and conformation changes of RC

The final goal of the studies of the fluorescence induction is to translate the observed characteristics of the kinetics into physico-chemical and physiological parameters of the system. The theory of fluorescence induction of antenna containing species (mainly for PS II) has been elaborated in great details including three major transitions of the RC: photochemistry ($PQ \rightarrow P^+Q^-$), radical-pair mechanism ($P^* \leftrightarrow P^+Bpheo^-$) and restricted transfer of excitation energy from closed RC to an open RC (Lavergne and Trissl 1995). From the shape of the induction curve, the functional absorption cross-section and connectivity of the photosynthetic complexes, from the relative yield of fluorescence, F_v/F_0, the quantum yield of primary charge separation and from the rate of the photochemical rise, the efficiency of light harvest by the photosynthetic units can be determined. Similar phenomenological models for RC (without antenna) have been established (Zankel et al. 1968; Osváth et al. 1996) but a thorough understanding of connection between fluorescence induction and redox and conformation reactions in the RC is still missing.

The observed fluorescence in isolated RC can arise from one BChl dimer (P), two BChl monomers and some residual (unknown) pigments left after protein purification. If the RC is open (PQ_AQ_B) or P^+ is re-reduced by an external electron donor ($P(Q_AQ_B)^-$), the dimer will be ready to absorb photon and emit fluorescence. If, however, P is oxidized ($P^+Q_A^-$ or $P^+Q_B^-$), it cannot be excited anymore and will not emit fluorescence. The BChl monomers play an accessory role in the fluorescence induction. They contribute to the more efficient capture of the light excitation (open RC) and/or to the observed fluorescence (closed RC). In open RC, the monomers increase the absorption cross-section of the RC and transfer the electronic excitation energy to the closely placed dimer. If P is oxidized, the BChl monomers may emit the electronic excitation energy in form of fluorescence.

The different redox states alone, however, cannot account for the complex kinetics of the fluorescence yield, because long after formation of the redox states of the RC, additional fluorescence changes occur that stretch over several orders of magnitude in time (Fig. 4A). We attribute these modifications of the yield to conformation changes of the RC (from "hot" to "relaxed" states via multiple equilibria). There is a wealth of information about experiments published in the literature, which support this interpretation. During prolonged illumination generating the trapped $P^+Q_A^-$ state, slow changes of the conformations were observed that converted the initial (hot) state to so-called "long living states" (LLS) (Kálmán and Maróti 1997; Mueh 1997; Mourik 2001; Andréasson and Andréasson 2003; Gouscha 2004; Agostiano 2005). Depending on the charge (redox) state of Q_A, two different protein conformations (with possible different dipoles) were identified (Katona et al. 2005). Recently, Breton et al. (2007) demonstrated the disappearance of the unusual C=O stretch in a revertant of the M260AW mutant indicating its possible involvement in redox and conformation events in Q_A. Computational studies also showed different H-bonding pattern in RC (Ishikita and Knapp 2005). These conformational changes were slow and linked to substantial proton uptake and release by residues near key electron transfer sites and pathways. Delayed fluorescence (Ogrodnik et al. 1999; Filus et al. 2004) and temperature-dependent charge recombination studies (McMahon et al. 1998) revealed similar dynamics of the RC on much shorter time scale. Our experiments discovered effects that might occur in overlapping time domains.

A minimal model for combination of light-induced redox and conformation reactions in RC is demonstrated in Scheme 1. After light excitation (rate constant k_I), the $P^+(Q_AQ_B)^-$ charge-separated state can undergo additional redox reactions, either by recombination to the initial state PQ_AQ_B (rate constant k_r), or (if external donor is present) by re-reduction of P^+ to $P(Q_AQ_B)^-$ (rate constant k_d). Both

$$\mathbf{PQ_AQ_B} \underset{k_r}{\overset{k_I}{\rightleftharpoons}} \mathbf{P^+(Q_AQ_B)_{hot}^-} \rightarrow \cdots \rightarrow \cdots \rightarrow \mathbf{P^+(Q_AQ_B)_{relaxed}^-}$$
$$\downarrow k_d \qquad\qquad k_c(t)$$
$$\mathbf{P\ (Q_AQ_B)_{hot}^-} \rightarrow \cdots \rightarrow \cdots \rightarrow \mathbf{P\ (Q_AQ_B)_{relaxed}^-}$$
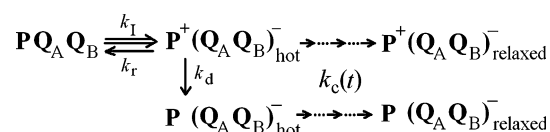
Scheme 1 Redox reactions combined with conformational relaxation via multiple equilibria in RC exposed to laser diode illumination. The monomolecular rate constants of photochemistry, charge recombination and electron donation to P^+ are k_I, k_r and k_d, respectively. The Kohlrausch relaxation involves time-dependent rate constant of $k_c(t) = k_o \cdot \alpha \cdot (k_ot)^{\alpha-1}$

$P^+(Q_AQ_B)^-$ and $P(Q_AQ_B)^-$ redox ("hot") states decay via several intermediates to final ("relaxed") states on extended time range. As the kinetics are clearly non-exponentials with lack of characteristic time scale (Fig. 4A), we utilize here the so-called "energy landscape" description that has been successfully used to explain protein dynamics (Ogrodnik et al. 1999; Filus et al. 2004), ligand binding, allosteric effects in enzyme function and protein folding (Osváth et al. 2006). To find the kinetics between the final (relaxed) and initial (hot) states, proper scaling relations should be used. If the amplitudes (a_n) and time constants (τ_n) of the Debye contributions of the intermediate level n of the multiple equilibria can be expressed as $a_n = a_1 \cdot \alpha^{n-1}$ ($0 < \alpha < 1$) and $\tau_n = \tau_1 \cdot n^\chi$ ($\chi > 1$) and n is extended to infinity ($n \to \infty$), then the kinetics can be approximated by the Kohlrausch relaxation function (stretched exponential): $\exp(-k_o \cdot t)^\alpha$ (Klafter and Shlesinger 1986). Here k_o is a characteristic rate constant and α is the stretching exponent which shows the deviation of the relaxation from the mono-exponential behavior ($\alpha = 1$).

The observed relative yield of fluorescence (F_v/F_0) can be considered as the sum of yields of the different ($i = 1,...,5$, see Scheme 1) redox and conformation states of the RC (φ_i) weighted by the corresponding concentrations of the protein ($[RC]_i$):

$$\frac{F_v}{F_0} = \frac{\sum_i \varphi_i \cdot [RC]_i}{\sum_i [RC]_i} \tag{5}$$

To simulate the measured kinetics and yields of fluorescence of the RC (Fig. 4A), the concentrations of the different states of the RC ($[RC]_i$) are derived from Scheme 1 with rate constants (k_r and k_d) determined from our experiments (Fig. 4B) and the corresponding fluorescence yields (φ_i) and kinetic parameters (k_I, k_o and α) are treated as fitting parameters. The fitted relative fluorescence yields are summarized in Table 1.

Whereas the increase of the fluorescence yield in the presence of donor is governed by the rate of the electron

donation to P^+ (k_d), the decrease in its absence is controlled by the light intensity (k_I) (Fig. 4A). Because the two rate constants were commeasurable in our case ($k_I = 1,800$ s^{-1} and $k_d = 330$ s^{-1}), a shallow dip could be observed in the kinetics. One of the most intriguing observations is the existence of non-exponential kinetics following the photochemical phase. The stretched exponential kinetics observed in fluorescence indicates hierarchical structures in the energy landscape of the protein.

The novelty of our observation is the short time range where the initial signs of complex conformation changes can be discovered. The conformation changes that have been reported so far are mostly induced by long illumination. Here we showed that the fastest components of the complex relaxation kinetics ($k_o = 1,000$ s^{-1}) could be as fast as the photochemistry or redox reactions and the conformational changes stretch over broad time scale ($\alpha = 0.30$). Our study indicates the potential use of fluorescence induction to reveal slight and early alterations of conformation in proteins.

Table 1 Relative fluorescence yields of RC (φ_i) in different redox and conformation states determined by fit of the kinetic traces (Fig. 4A) based on Scheme 1 and Eq. (5)

RC_i	Redox states	Conformation states	
		Hot state	Relaxed state
1	PQ_AQ_B	N.D.[a]	1.00
2	$P^+Q_A^-$/terb	0.49	0.30
3	$P^+Q_B^-$	0.66	0.40
4	PQ_A^-	2.50	3.80
5	PQ_B^-	N.D.	N.D.

[a] *N.D.* not determined

References

Andréasson U, Andréasson L-E (2003) Characterization of a semistable, charge-separated state in reaction centers from *Rhodobacter sphaeroides*. Photosynth Res 75:223–233

Agostiano A, Milano F, Trotta M (2005) Trapping of a long-living charge separated state of photosynthetic reaction centers in proteoliposomes of negatively charged phospholipids. Photosynth Res 83(1):53–61

Borisov AYu, Godik VI (1972) Energy transfer to the reaction centers in bacterial photosynthesis. II. Bacteriochlorophyll fluorescence lifetimes and quantum yields for some purple bacteria. J Bioenerg Biomembr 3(6):515–523

Breton J, Lavergne J, Wakeham MC, Nabedryk E, Jones M (2007) The unusually strong hydrogen bond between the carbonyl of Q(A) and his M219 in the *Rhodobacter sphaeroides* reaction center is not essential for efficient electron transfer from Q(A)(−) to Q(B). Biochemistry 46:6468–6476

Cogdell RJ, Isaacs NW, Freer AA, Howard TD, Gardiner AT, Prince SM, Papiz MZ (2003) The structural basis of light harvesting in purple bacteria. FEBS Lett 555:35–39

Cser K, Vass I (2007) Radiative and non-radiative charge recombination pathways in Photosystem II studied by thermoluminescence and chlorophyll fluorescence in the cyanobacterium *Synechocystis* 6803. Biochim Biophys Acta 1767:233–243

De Klerk H, Govindjee, Kamen MD, Lavorel J (1969) Age and fluorescence characteristics in some species of athiorhodaceae. Proc Natl Acad Sci USA 62:972–978

Dau H (1994) Molecular mechanisms and quantitative models of variable Photosystem II fluorescence. Photochem Photobiol 60(1):1–23

Filus Z, Laczkó G, Wraight CA, Maróti P (2004) Delayed fluorescence from photosynthetic reaction center measured